This is the last draft sent to the Editorial by the authors of the article:

M. GÓMEZ, C. I. GARCIA, D. M. HAEZEBROUCK, A. J. DEARDO
"Design of Composition in (Al/Si)-alloyed TRIP Steels"

ISIJ International
Vol. 49 (2009), Pages: 302-311
DOI: 10.2355/isijinternational.49.302
ISSN: 0915-1559

Design of composition in (Al/Si)-alloyed TRIP Steels

Manuel GOMEZ[1)], C. Isaac GARCIA[2)], Dennis M. HAEZEBROUCK[3)], Anthony J. DEARDO[2) 4)]

1) Formerly in BAMPRI, University of Pittsburgh, now in National Center for Metallurgical Research (CENIM-CSIC), Avda. Gregorio del Amo 8, 28040 Madrid, Spain

e-mail: mgomez@cenim.csic.es

2) Basic Metals Processing Research Institute (BAMPRI), Mechanical Engineering and Materials Science Department, University of Pittsburgh, 848 Benedum Hall, Pittsburgh, PA 15261, USA

e-mail: garcia@engr.pitt.edu, deardo@engr.pitt.edu

3) United States Steel Corporation, Research and Technology Center, Munhall, PA 15120, USA.

e-mail: DMHaezebrouck@uss.com

4) Distinguished Professor, Mechanical Engineering, Oulu University, Finland.

There is an increasing interest in the progressive substitution of Si by Al in TRIP steels in order to obtain alloys with excellent mechanical properties and improved coatability. In this paper, thermodynamic calculations have been carried out with the help of JMatPro™ software in order to assess and compare the effects that Si and Al additions exert on the phase transformation, carbon enrichment and alloying element content of phases during continuous galvanizing of multiphase steels. These simulations have provided important implications regarding the optimal combination of Si and Al. It has been found that Al causes a more pronounced increase of A_3 temperature and a wider extension of the intercritical range than Si. For a constant volume fraction of phases, the carbon content in austenite is similar for Al and Si-alloyed steels. However, ferrite in Al-alloyed is richer in carbon and consequently an increase in its strength could be expected. The hardenability of intercritically annealed austenite has been estimated for alloys with different combinations of Mn, Al and Si. Finally, simulated CCT diagrams predict for Al-alloyed steels a higher amount of new ferrite formed during cooling from intercritical annealing and the need of shorter isothermal holding times at 460 ºC. However, Si-TRIP steels would need faster cooling rates to prevent pearlite formation and longer isothermal holding times to complete the bainitic transformation and to obtain a microstructure with high retained austenite.

KEY WORDS: TRIP steel, aluminum, silicon, thermodynamic calculations, phase transformation, carbon content in phases, continuous galvanizing.

1. Introduction

Silicon is the most significant element traditionally used [1-3] to originate the TRIP effect (strain induced transformation of retained austenite into martensite) [4] in steels. This element is thought to inhibit the precipitation of cementite and thereby enhances the stabilization of austenite (decrease of Ms temperature below room temperature) thanks to the carbon rejected from the bainitic ferrite that is assumed to form during isothermal holding at low temperatures. In order to achieve the austenite stabilization some authors have used CMnSi TRIP-aided steels with Si contents above 1.5% [5-8]. However, in selecting steels for coated applications, it is important to pay attention to the silicon content, as high Si additions are known to cause galvanizing problems [9] and it is generally accepted that a level of Si above 0.5% will hinder coating [10]. Concretely, Si forms a very strong and adherent layer of complex manganese-silicon-oxides, which is easily rolled into the surface during hot rolling and is difficult to be removed. This leads to poor coatability so bare spots can appear eventually on the sheet surface [10,11].

Manganese can also be used to produce adequate amounts of retained austenite and improve the mechanical properties of TRIP steels, but Mn levels above 2% may also degrade coatability, even in the absence of Si [10]. Some authors [10,11] have studied the galvanizing behavior of steels where Si was partially or fully substituted by other elements that are known to cause the TRIP effect such as P or Al. The addition of relatively high levels of P (up to 0.1%) gives satisfactory galvanizing results. Phosphorus is useful for solid solution strengthening [12,13] and P-TRIP steels have shown interesting microstructural characteristics and mechanical properties [9,14]. However, it has been shown that P additions slow galvannealing kinetics [15] and can lead to cold work embrittlement [16] for low C contents.

According to some authors, Al as a solute element does not segregate to the surface during intercritical annealing before galvanizing [17], so Al additions are not expected to influence the coatability adversely [18]. In fact, it has been found that steels with contents of up to 1.5% Al can be successfully galvanized [10,19,20]. Mahieu et al. found that Al, like Si, form iron-aluminum-oxides, but these do not affect the coatability of low-Si steels [11]. On the contrary, Al has the ability to prevent Si from segregating to the surface. When Si is replaced by Al, a Fe-Al spinel is formed at the surface. That spinel does not deteriorate galvanizability and inhibits the formation of detrimental Mn_2SiO_4 [11].

Aluminum is a strong ferrite stabilizer and it is not soluble in cementite [21]. Al effectively inhibits the formation of cementite during the alleged bainite transformation as it acts to lower the activity of C in the carbon enriched pools in austenite. Hence, Al is helpful for the retention of austenite at room temperature and the optimization of the TRIP effect during straining [22]. The effect of the partial or full substitution of Si by Al on the microstructure and mechanical properties of CMn TRIP steels has been studied by several authors [22-28]. Excellent mechanical properties have been found and Al alloyed TRIP steels are presented as promising candidates for processing in continuous galvanizing lines due to their lower Si contents. Besides, several authors have noted that Al TRIP steels need shorter holding times (less than 60 s at temperatures of 450-465 ºC) than Si steels to obtain maximal values in the amount of retained austenite and optimal values of mechanical properties [12,23,25,26,28]. This is an important advantage for their industrial processing in continuous annealing lines. On the other hand, when two different Al levels have been compared, the steel with higher Al content has presented a higher ductility for identical strength levels [22]. In dual-phase steels, Al additions increase the balance of total elongation and tensile strength due to the refined ferrite structure and morphology of martensite [29].

However, at a constant elongation value, Si-TRIP steels usually present higher tensile strengths than Al compositions due to the much more significant solid solution strengthening effect of Si compared to Al [12,13,26,30,31]. It has been proposed that Si level must be > 0.8% to obtain a reasonable amount of retained austenite [10]. Nonetheless, steels with 0.4% Si and without Al have shown remarkable mechanical properties [1], thanks to the combination of TRIP effect and a "composite" strengthening effect [3,32,33]. Several authors have concluded that full substitution of Si by an equivalent amount of Al would yield to a poorer strength ductility/balance; hence, they recommended the use of a mixed Al–Si TRIP-assisted multiphase steel. This type of steel would be an efficient compromise between the processing practice of these steels, the resulting mechanical properties and the industrial requirements [22,26].

In conclusion, efforts are being made in the progressive substitution of Si by Al in TRIP steels in order to obtain alloys with excellent mechanical properties and better coatability. The work described in this paper presents some design concepts based on thermodynamic calculations made with the specific simulation software JMatPro™. The main aim of this work was to assess and compare the effect of Si and Al additions on the phase transformation and carbon enrichment of phases during the intercritical annealing of the steel and its subsequent cooling to isothermal holding temperature associated with the continuous galvanizing of TRIP steels. The alloy design and the thermal simulations could provide very helpful tools for the definition of optimal combinations of Si and Al to obtain the desired TRIP effect without hindering the galvanizability of the steel.

2. Experimental Procedure

To carry out the thermodynamic simulations, JMatPro™ software (version 4.0) was used in all cases. JMatPro™ (acronym for "Java-based Materials Properties") is a Calphad-type software package for calculating and simulating the physical and thermophysical properties and behavior of multicomponent metallic systems [34]. This software has been extensively used with proven accuracy to simulate precipitation [35], phase transformations and CCT diagrams [36,37], solidification properties and high temperature strength [38,39], among other physical phenomena and properties. To make the calculations in this paper, the program was coupled with Fe-DATA thermodynamic database [40]. The calculations were made under equilibrium conditions, except for the case of continuous cooling transformation (CCT) diagrams. First of all, to study the effect of Si or Al additions on the transformation lines of the Fe-C diagram, the series of chemical compositions shown in **Table 1** was selected. The C content was varied between 0% and 0.9 wt. % to build this region of the phase diagram whereas the Mn amount was kept at a constant value of 1.5%, typical of many commercial steels. The amounts of Si and Al were also varied within the range presented in the table (0%-1.5%). To study the effect of Si or Al additions on the volume fractions and carbon contents of the phases (austenite and ferrite) formed during intercritical annealing in a simple Fe-C-Mn system, the bulk carbon content was fixed at 0.15% C. In this case, the amounts of Si and Al were varied again within the range (0%-1.5%). The partitioning of alloying elements (Al or Si) during phase transformation was also studied for Fe-0.15%C-1.5%Mn alloys.

On the other hand, the chemical composition presented in **Table 2** was used to obtain conclusions more applicable to real TRIP or DP steels. The values of volume fraction, carbon content and hardenability of intercritical austenite were calculated for different binary combinations of Mn-Si-Al within the ranges presented in the table. The carbon equivalent (CE) was used to estimate the hardenability during intercritical annealing of steels with

several amounts of Mn, Si and Al. The value of CE was determined by using Equation (1) from the International Institute of Welding (IIW) where Si is taken into account [41].

$$CE = \%C + \left(\frac{\%Mn + \%Si}{6}\right) + \left(\frac{\%Cr + \%Mo + \%V}{5}\right) + \left(\frac{\%Cu + \%Ni}{15}\right) \quad (1)$$

The hardenability of intercritically annealed austenite was also estimated for several compositions by calculating the value of ideal critical diameter (DI) according to ASTM A255-07 standard [42].

Continuous cooling transformation (CCT) diagrams of steels of **Table 2** were plotted for the specific case of 1.5%Mn and an addition of 1% Al or 1% Si. An intercritical reheating temperature corresponding to a 50% ferrite / 50% austenite phase balance was chosen to simulate the diagram. Based on experimental observations with similar steels and processing conditions [28], the value of initial intercritical austenite grain size considered was equal to ASTM-12 (i.e. about a mean linear intercept length of 5 microns).

3. Results and Discussion

Figures 1 and **2** show, respectively, the effect of Al and Si additions on the Fe-C-1.5%Mn phase diagram. It can be clearly seen that Al causes a much more pronounced increase of A_3 temperature than the same amount of Si. In both cases, a similar slight increase of A_1 is observed, as shown in **Figures 1b** and **2b** for the specific case of a Fe-0.15%C-1.5%Mn alloy. As a result, the region (A_3-A_1) is considerably wider in Al alloyed steels than in those with the same amount of Si. This expansion of the intercritical region caused by Al has been described as greatly beneficial in enhancing process stability during continuous annealing [29,43] as it decreases the sensitivity of the balance of phases and mechanical

properties to the variations in annealing temperature. However, it must be mentioned that the temperature necessary for a hypothetical intercritical anneal leading to a 50% ferrite / 50% austenite phase distribution (see **Figures 1b** and **2b**) would be higher in Al TRIP steels.

The reduced sensitivity of the balance of phases to the variations in annealing temperature can be evaluated in **Figure 3**. In a 0.15%C alloy, the austenite volume fraction of steels with an Al content near 1% will vary between 28% for an intercritical annealing temperature (IAT) of 750 ºC and 63 % when IAT=850 ºC. However, the same amount of Si can make the austenite volume fractions to vary between 34% and 100%. Obviously, the relative changes in ferrite volume fraction (**Figure 4**) with temperature will take an analogous trend.

Al and Si displace the A_3 line of the Fe-C diagram to higher temperatures and to the right side, which indicates a higher solubility of carbon in austenite during intercritical annealing. This can be verified in **Figure 3**, which shows how, at equal temperature, austenite in Al alloyed steels will have higher carbon content than in steels where Si is added to cause the TRIP effect. **Figure 4** shows that the carbon content of the intercritically annealed ferrite follows a similar trend, i.e., at the same temperature, Al steels will also have a stronger carbon enrichment of ferrite than Si steels.

Figure 5 presents the evolution of carbon content in austenite and ferrite as a function of the amount of Al or Si for the particular case of IAT=800 ºC. Both elements cause an increased carbon enrichment of the phases present during intercritical annealing, but this effect is stronger for the case of Al additions. The carbon enrichment of austenite at the end of intercritical annealing is a critical factor for the hardenability of the steel and the likelihood of having martensite and/or stable retained austenite at room temperature after processing. On the other hand, the carbon content of the ferrite formed during cooling is crucial for the solid solution strengthening effect. Nevertheless, in many cases the temperature used in industrial

processing will not be the same for all the steels, but it will depend on the balance of phases required for the DP or TRIP steel. **Figure 6** presents again the evolution of carbon content in austenite and ferrite as a function of Al or Si content, but now the temperatures considered have been calculated to obtain a theoretical phase distribution with 50% or 70% ferrite after annealing. In **Figure 6a** it can be verified that, although the value of carbon in austenite is slightly higher for Si alloys, the state of austenite (combination of volume fraction and carbon content) at the end of intercritical annealing of the model Fe-0.15%C-1.5%Mn alloy studied would be nearly identical, no matter whether the alloying element were Al or Si. However, it is found that, for the same balance of phases (50% or 70% ferrite), Al steels will have a more pronounced carbon enrichment of ferrite compared to Si steels (**Figure 6b**).

Figure 7 compares, for the case of 1% Al or Si additions, the balance and carbon content of phases formed during cooling from 1000 ºC to 400 ºC under equilibrium conditions. It can be seen how at any temperature the amount and carbon content of ferrite are higher for the case of Al alloying. Conversely, the austenite is richer in carbon but its volume fraction is lower for the case of Al alloying. These differences help to explain the different behaviors shown in **Figures 6a** and **6b**.

Figure 8 shows the distribution of Al and Si in ferrite and austenite within the intercritical range during a cooling in equilibrium for 1% additions of Al or Si. The partitioning of Si would start at a lower temperature and would occur during a narrower temperature interval. Higher contents of Al in ferrite can be expected at any temperature, whereas the austenite would remain richer in Si compared to Al. This is true for any intercritical temperature and any Al or Si content, as can be seen in **Figure 9**, which represents the Al/Si contents in austenite for temperatures corresponding to 50% or 70% ferrite. It should be taken into account that processing of TRIP steels involves short intercritical annealing times and fast cooling rates. Phase transformation is usually considered

as a paraequilibrium process in which the diffusivity of the substitutional species is negligible compared to that of interstitial species [44]. Therefore, values in **Figures 8** and **9** should be considered as an estimate to indicate the tendency toward compositional adjustment with obvious kinetic restrictions. On the other hand, the maximum solubility of Al in pure gamma-iron has been reported to vary between 0.6% [45] and 1-1.5% [29], whereas the solubility in alpha iron could reach about 30% [45].

Figure 10 shows that, compared to Si, the addition of Al to the steel causes a higher solubility of carbon in ferrite both within the intercritical and subcritical regions. Taking an amount of 1% of Al or Si, the maximum solubility of C would be 0.011% for the case of Al and 0.0075% for Si additions. These results and those shown in **Figure 7d** are interesting as they permit to expect that the ferrite formed during cooling from IAT to isothermal holding in galvanized TRIP steels (at temperatures close to 460 ºC) will be richer in carbon when the alloying element is Al instead of Si. Si provides a much stronger solid solution strengthening effect than Al [13,30], but it should also be considered that the ferrite in Al steels can be richer in carbon and this could partially compensate the strength values. The solid solution strengthening coefficient of Si (measured as the increase in the value of yield strength) is about 83 MPa per 1 wt% in solution. However, the coefficient of C is about 5000 MPa per 1wt % [46]. Therefore, for a constant balance of phases, a slight difference of 35 ppm in ferrite carbon content as that shown in **Figure 10** would theoretically lead to an increase in yield strength of 18 MPa for the Al addition.

The chemical compositions presented in **Table 2** (that are similar to commercial TRIP steels) were used to calculate, at a constant temperature of 800 ºC, the values of austenite volume fraction, carbon content, carbon equivalent and ideal diameter for different combinations of Mn-Si-Al (**Figure 11**). Observing the evolution of austenite volume fraction (first row of **Figure 11**), the austenite stabilizing effect of Mn can be perceived in these

figures, while Si and especially Al, act as ferrite stabilizing elements. The respective effect of these three elements on the austenite carbon content at 800 ºC is analogous: Al causes stronger carbon enrichment than Si, but Mn additions lead to lower austenite carbon concentrations. The most interesting results come from the comparison of hardenability values. Al is not explicitly included in Equation (1) used to estimate the value of CE. However, the strong carbon enrichment of the austenite provoked by Al would cause an "indirect" effect of increasing the hardenability of the fraction of intercritical austenite present at 800 ºC. Observing the maps of CE values built from Mn-Si-Al combinations, it is found that both Si and Al bring about a higher relative increase in CE than Mn, although the fraction of γ would increase with Mn. The evolution of hardenability expressed by DI values is very similar to that of CE values, as seen in the last row of **Fig. 11**. The increase in DI due to Si additions is slightly stronger than the effect of Al, as a specific hardenability multiplying factor for Si is considered in the ASTM standard [42)], but this does not happen for Al. The effect of Mn on DI is lessened by the associated drop in carbon content of intercritical austenite. As shown in **Figure 12a**, the CE of austenite at 800 ºC and with 1.5%Mn bulk content would be slightly higher for Si additions than for the same amount of Al. However, if an intercritical temperature corresponding to 50% γ is considered, Si steels offer quite higher and increasing values of CE, whereas Al additions bring about a decrease in these values. This is due to the explicit effect of Si introduced in Equation (1) and also, to some extent, to the lower values of T_{50} for Si additions that cause higher values of C, Mn, Cr and Mo in solution compared to Al steels. It should be mentioned that in other equations used to calculate CE the coefficient for Si is lower or even it does not appear [47)]. Aluminum has traditionally been considered as an element with negligible effect on hardenability [47,48)]. Grossman affirmed that aluminum could be a powerful alloying element for hardenability[49)], but the content of Al in steel has been usually very low and therefore references about a direct influence of Al on

hardenability are scarce. According to Adrian [50] there is no experimental evidence that Al itself increases the value of this parameter, but this element can enhance the hardenability of vanadium treated steels because it promotes the formation of clusters consisting of substitutional atoms with a high chemical affinity for the interstitial atoms, and this changes the properties of the austenite matrix.

Figure 12b shows the evolution of hardenability of intercritical austenite at 800 ºC and at temperature corresponding to (50% α / 50% γ) versus Al or Si bulk content, expressed by the value of ideal diameter (DI). This plot is very similar to the results for CE shown in **Fig. 12a**. As mentioned above, the explicit effect of Si on the value of DI has been taken into account according to the standard, but this is not the case for Al. As can be seen in **Fig. 12c**, both ways of estimating hardenability (CE and DI) follow a practically linear relationship for the range of compositions studied.

Finally, CCT diagrams were simulated for the steel of **Table 2** with 1.5%Mn and considering an intercritical reheating temperature corresponding to a 50% ferrite / 50% austenite distribution. For practical purposes, a hypothetical processing schedule consisting of a typical cooling rate of 15 ºC/s from intercritical temperature followed by an isothermal holding of 1 min at Zn bath temperature (460 ºC) has been included in the figures. **Figure 13a** shows the CCT diagram of a steel without Al or Si. When 1%Al is added to steel (Fig. 13b), the curve of ferrite formation is displaced more than one order of magnitude to shorter times. If the alloying element addition is 1% Si (Fig. 13c) the acceleration of ferrite formation would be much less pronounced. **Figure 13d** shows together the curves of ferrite formation from an intercritical temperature of (50% α / 50% γ) for the three compositions. As indicated in **Fig. 13d**, ferrite formation during cooling would start at shorter times and higher temperatures (1 s, 812 ºC) in an Al-alloyed TRIP steel than for the case of Si-additions (11 s, 618 ºC) or a CMn chemistry (13 s, 565 ºC). This is in agreement with the values of CE and DI shown in

Figure 12. It has been found that, compared to fully austenitization, the intercritical annealing of the steel can drastically accelerate the formation of "new ferrite" (despite the significantly higher carbon content and hardenability of austenite), due to the presence of pre-existing austenite/ferrite phase boundaries [29,51-54]. During cooling, these interfaces only need to grow epitaxially and the step of nucleation is not required. According to **Figure 13**, ferrite formation during cooling from IAT to isothermal holding (IH) would be almost unavoidable in Al-steels and the amount of "new ferrite" formed should be higher in Al steels than for Si steels. Extensive formation of new ferrite in Al-TRIP steels has previously been described by several authors [23,28,29,53]. Besides, Suh et al have shown that partial replacement of Si by Al encourages the conversion of intercritical austenite to ferrite during cooling from intercritical annealing [55].

Figure 13 also shows that Si-TRIP steels have a higher risk of pearlite formation during cooling near 10-15 ºC/s. This agrees with results from other authors [54,56] and indicates that Si-steels would need faster cooling rates in order to prevent a decrease in the carbon content of untransformed retained austenite that would reduce the amount of retained austenite in final microstructure [57]. However, the content of retained austenite of Al-steels is hardly influenced by the cooling rate [57]. On the other hand, the curves of bainite formation are displayed at shorter times and higher temperatures in the case of Al additions. If the CCT diagrams were used to give an approximation of the isothermal transformation at 460 ºC after cooling at 15 ºC/s, it would result that an isothermal holding time (IHt) of 44 s would be long enough to reach the curve that denotes the end of bainite formation (Bf) in the 1% Al steel, as this curve is intersected at an approximate time of 68 s when T = 460 ºC (see **Fig. 13b**). However, a steel with 1% Si would need an IHt longer than 7 min at 460 ºC to reach the end of bainitic transformation, as Bf curve is found near 460 s after the end of intercritical annealing IAT, as shown in **Fig. 13c**. The time for the end of bainite formation in the Si-TRIP

steel is the longest among the three compositions studied, as the steel without Al-Si additions needs about 1 min at 460 ºC to reach Bf (**Fig. 13a**). To sum up, the bainitic transformation (that according to theory contributes to the carbon enrichment and stabilization of austenite) would need much shorter IH times to be completed in Al-TRIP steels compared to Si steels. This is an important practical conclusion that coincides with experimental observations that show that Si-TRIP steels require continuous galvanizing routes with long austempering times (3-5 min) at 400-500 ºC to maximize retained austenite content and mechanical properties [12,54]. However, Al-TRIP steels can be satisfactorily processed with temperatures closer to the zinc bath (460 ºC) and much shorter IH times [12,23,25,26,28].

It has been previously mentioned that it is generally accepted that a level of Si above 0.5% will hinder coating[10]. The variable degree of reactivity of silicon with the zinc coating can originate the phenomenon known as "Sandelin effect" [58,59], which is in the origin of coatability problems. According to the theory of this phenomenon, the optimal galvanizability is obtained for Si contents below 0.03%. However, this phenomenon reaches its maximum peak at 0.07% Si, decreases for higher Si contents and it grows again at Si>0.3% [59]. This means that supplementary efforts to restrict Si to the lowest content might be unnecessary or even detrimental, as a silicon content in the approximate range (0.1%-0.3% Si) should be suitable for many industrial applications. The latter means that the solid solution strengthening effect of Si [13,30] could be exploited to some extent without damaging coatability significantly. This detail can be taken into account when using maps like those shown in **Fig. 11**.

4. Summary and Conclusions

With the help of JMatPro^{TM} software, thermodynamic calculations have been made to assess and compare the effect that Si and Al additions exert on the phase transformation, carbon enrichment and alloying element content of phases during the intercritical annealing, cooling and isothermal holding of TRIP and DP steels. These simulations can provide a very helpful tool for the design of improved combinations of Si and Al to obtain the desired TRIP effect without hindering the galvanizability of the steel.

It has been found that Al causes a more pronounced increase of A_3 temperature and a wider extension of the intercritical range compared to Si, which can be beneficial for process stability during intercritical annealing. When an intercritical temperature corresponding to a constant fraction of $\alpha \rightarrow \gamma$ transformation is considered, the values of carbon content in austenite for Al and Si-alloyed steels are similar, but the values of %C in ferrite are higher for the case of Al additions. The stronger carbon enrichment of ferrite in Al steels during annealing and subsequent cooling could partially compensate for the significant solid solution strengthening effect of Si additions. Under equilibrium conditions, higher contents of Al in ferrite could be expected at any temperature, whereas the enrichment of austenite in Si would be stronger.

The carbon equivalent and ideal diameter of the intercritically annealed austenite have been determined for different combinations of Mn, Al and Si. At a constant temperature, the carbon enrichment of austenite caused by Al may act as an "indirect" way of increasing hardenability of steel. However, the values of CE and DI at a constant fraction of transformation are higher for Si than for Al additions. It is found that the values of CE and DI follow very similar trends versus compositional changes.

Finally, simulated CCT diagrams predict for Al-alloyed steels a higher amount of new ferrite formed during cooling from intercritical annealing and the need of shorter isothermal holding times at 460 ºC. However, Si-TRIP steels would need faster cooling rates to prevent

pearlite formation and longer isothermal holding times to complete the isothermal bainitic transformation.

Acknowledgments

Dr. Gomez acknowledges financial support of his Postdoctoral Fellowship in BAMPRI, University of Pittsburgh from the Spanish Ministry of Education and Science and to the Fulbright Scholar Program. The authors are also grateful for the financial support of this work by BAMPRI and its industrial and governmental sponsors.

Disclaimer

The material in this paper is intended for general information only. Any use of this material in relation to any specific application should be based on independent examination and verification of its unrestricted availability for such use, and determination of suitability for the application by professionally qualified personnel. No license under any patents or other proprietary interest is implied by the publication of this paper. Those making use of or relying upon the material assume all risks and liabilities arising from such use or reliance.

REFERENCES

1) P. J. Jacques, E. Girault, P. Harletz and F. Delannay: *ISIJ Int.*, **41** (2001), 1061.

2) R. Petrov, L. Kestens and Y. Houbaert: *ISIJ Int.*, **41** (2001), 883.

3) P. Jacques, X. Cornet, P. Harlet, J. Ladriere and F. Delannay: *Metall. Mater. Trans A*, **29A** (1998), 2383.

4) V. F. Zackay, E. R. Parker, D. Fahr and R. A. Busch: *ASM Transactions Quarterly*, **60** (1967), 252.

5) J. Huang, W.J. Poole and M. Militzer: *Metall. Mater. Trans. A*, **35A** (2004), 3363.

6) M. R. Berrahmoune, S. Berveiller, K. Inal, A. Moulin and E. Patoor: *Mater. Sci. Eng. A*, **378** (2004), 304.

7) S. J. Kim, C. G. Lee, T. H. Lee and C. S. Oh: *Scripta Mater.*, **48** (2003), 539.

8) C. G. Lee, S. J. Kim, T. H. Lee and C. S. Oh: *ISIJ Int.*, **44** (2004), 737.

9) L. Barbé, K. Verbeken and E. Wettinck: *ISIJ Int.*, **46** (2006), 1251.

10) B. Mintz: *Int. Mater. Rev.*, **46**, (2001), 169.

11) J. Mahieu, B. C. De Cooman, J. Maki and S. Claessens: *Iron Steelmaker*, **29** (2002), 29.

12) R. Pradhan and J. P. Wise: 45th MWSP Conf Proc, ISS, Vol XLI, (2003), 153.

13) F. B. Pickering: Physical Metallurgy and the Design of Steels, Applied Science Ltd, London, (1978), 4.

14) H.C. Chen, H. Era and M. Shimizu: *Metall. Trans. A*, **20A** (1989), 437.

15) I. Hertveldt, S. Claessens, and B. C. De Cooman: *Mater. Sci. Technol.* **17** (2001), 1508.

16) J.S. Rege, M. Hua, C.I. Garcia and A.J. Deardo: *ISIJ Int.*, **40** (2000), 191.

17) M. De Meyer, B.C. De Cooman and D. Vanderschueren: *Iron Steelmaker* **27** (2000), 55.

18) J. Mahieu, S. Claessens and B. C. De Cooman: 5th Int. Conf. on Zinc and Zinc Alloy Coated Steel Sheet (Galvatech 2001), Conf. Proc., Verlag Stahleisen, Düsseldorf, (2001), 644.

19) J. Maki, J. Mahieu, B. C. De Cooman, and S. Claessens: *Mater. Sci. Technol.*, **19** (2003), 125.

20) E.M. Bellhouse and J.R. McDermid: *Mater. Sci. Eng. A*, **491** (2008), 39.

21) A. Pichler, P. Stiaszny, R. Potzinger, R. Tikal and E. Werner: 40th MWSP Conf. Proc., ISS, VOL. XXXVI, (1998), 259.

22) P. J. Jacques, E. Girault, A. Mertens, B. Verlinden, J. Van Humbeeck and F. Delannay: *ISIJ Int.*, **41** (2001), 1068.

23) J.E. Garcia-Gonzalez, C.I. Garcia, M. Hua and A.J. DeArdo: Conf Proc. Materials Science and Technology MS&T'05, (2005), 3.

24) M. De Meyer, D. Vanderschueren and B. C. DeCooman: *ISIJ Int.*, **39** (1999), 813.

25) J. Mahieu, J. Maki, B.C. De Cooman, and S. Claessens: *Metall Mater. Trans A*, **33A** (2002), 2573.

26) E. Girault, A. Mertens, P. Jacques, Y. Houbaert, B. Verlinden and J. V. Humbeeck: *Scripta mater.* **44** (2001), 885.

27) K. Sugimoto, B. Yu, Y. Mukai and S. Ikeda: *ISIJ Int.* **45** (2005), 1194.

28) M. Gomez, C. Garcia, D. Haezebrouck and A. DeArdo: AIST Steel Properties and Applications Conf. Proc., Materials Science and Technology Conf. (MS&T), Detroit, (2007), 1.

29) O.A. Girina and N.M. Fonstein: Developments in Sheet Products for Automotive Applications, Conf Proc. Materials Science and Technology MS&T'05, (2005), 65.

30) W. C. Leslie: *Metall. Trans.*, **3** (1972), 5.

31) I. Tsukatani, S. Hashimoto and T. Inoue: *ISIJ Int.* **31** (1991), 992.

32) P.J. Jacques: *Curr. Opin. Solid State Mat. Sci.* **8**, (2004), 259.

33) P. J. Jacques, Q. Furnemont, S. Godet, T. Pardoen, K. T. Conlon and F. Delannay: *Philos. Mag.* **86** (2006), 2371.

34) N. Saunders, Z. Guo, X. Li, A.P. Miodownik and J.P. Schillé: JOM, **55** (2003), 60.

35) Z. Guo and W. Sha: *Mater. Sci. Eng. A*, **392** (2005), 449.

36) D.A. Akinlade, W.F. Caley, N.L. Richards and M.C. Chaturvedi. *Mater. Sci. Eng. A*, **486** (2008), 626.

37) A. Sullivan and J.D. Robson: *Mater. Sci. Eng. A*, **478** (2008), 351.

38) Z. Guo, N. Saunders, A.P. Miodownik and J.-Ph. Schille: *Mater. Sci. Eng. A*, **413–414** (2005), 465.

39) Z. Guo, N. Saunders, J.P. Schillé and A.P. Miodownik: *Mater. Sci. Eng. A* (2008), doi:10.1016/j.msea.2007.09.097.

40) N. Saunders and A.P. Miodownik: CALPHAD (Calculation of Phase Diagrams): A Comprehensive Guide, Pergamon Materials Series vol.1, ed. R. W. Cahn (Pergamon Press, Oxford, UK, (1998), 1.

41) H. K. D. H. Bhadeshia: Bainite in Steels, Institute of Metals, London (2001), 398.

42) ASTM Standard A 255-07, Annual Book of Standards, vol. 01.05, ASTM International, West Conshohocken, PA, (2008), 30.

43) N. Pottore, N. Fonstein, I. Gupta and D. Bhattacharya: MS&T'05 Proceedings, (2005), 97.

44) G. Ghosh and G.B. Olson: *Metall. Mater. Trans. A* **32A** (2001), 455.

45) E. C. Bain and H. W. Paxton: Alloying elements in steel, Ed. ASM, Metals Park, Ohio, (1961), 242-243.

46) T. Gladman: The Physical Metallurgy of Microalloyed Steels, Institute of Materials, London, (1997), 36.

47) ASM International: Metals Handbook, Ninth Edition, Vol. 15. "Casting", (1988), 533.

48) I. R. Kramer, S. Siegel, and G. Brooks: *Trans. AIME*, **167** (1946), 670.

49) M. A. Grossmann: *Trans. AIME*, **150** (1942), 227.

50) H. Adrian: *Mater. Sci. Technol*. **15** (1999), 366.

51) R. Priestner and M. Ajmal: *Mater. Sci. Technol.*, **3** (1987), 360.

52) J. Zrník, I. Mamuzić and S. V. Dobatkin: *Metalurgija* **45** (2006), 323.

53) N. Fonstein, O. Yakubovsky, D. Bhattacharya and F. Siciliano: *Mater Sci. Forum*, **500-501** (2005), 453.

54) N. Fonstein, N. Pottore, S. H. Lalam and D. Bhattacharya: Austenite Formation and Decomposition, ISS and TMS, (2003), 549.

55) D. W. Suh, S.-J. Park, C.-S. Oh and S.-J. Kim: *Scripta Mater.* **57** (2007), 1097.

56) B. Ehrhardt, T. Gerber, H. Hofmann and T. W. Schaumann: *Steel Grips*, **2** (2004), 247.

57) S. Traint, A. Pichler, K. Spiradek-Hahn, K. Hulka and E. Werner: Austenite Formation and Decomposition, ISS and TMS, (2003), 577.

58) R. Sandelin: *Wire and wire products*, **16** (1941), 28.

59) J. Foot, P. Perrot and G. Reumont: *Scripta Metall. Mater.*, **28** (1993), 1195.

LIST OF TABLE CAPTIONS

Table 1. Chemical composition of the Fe-C-Mn-Al and Fe-C-Mn-Si model alloys used to study by means of JMatPro^{TM} simulations the effect of Al and Si on the Fe-C-1.5% Mn phase diagram, the volume fractions of phases and the C, Al and Si contents in phases formed during annealing (wt%).

Table 2. Chemical composition of the model TRIP steel used to study by means of JMatPro^{TM} simulations the effect of Mn, Al and Si additions on the austenite volume fraction and carbon equivalent at 800 ºC (wt%).

LIST OF FIGURE CAPTIONS

Fig. 1. (a) Effect of Al additions (between 0% and 1.5% Al) on the transformation lines of Fe-C-1.5%Mn phase diagram; (b) Effect of Al on transformation temperatures for a Fe-0.15%C-1.5%Mn alloy. The temperatures represented are the austenite-ferrite transformation temperature (A_3), the temperature for a 50% austenite / 50% ferrite phase distribution and the eutectoid transformation temperature (A_1).

Fig. 2. (a) Effect of Si additions (between 0% and 1.5% Si) on the transformation lines of Fe-C-1.5%Mn phase diagram; (b) Effect of Si on transformation temperatures for a Fe-0.15%C-1.5%Mn alloy. The temperatures represented are the austenite-ferrite transformation temperature (A_3), the temperature for a 50% austenite / 50% ferrite phase distribution and the eutectoid transformation temperature (A_1).

Fig. 3. Comparison of the influence of Al and Si additions on austenite volume fraction and carbon content at 750 ºC, 800 ºC and 850 ºC for a Fe-0.15%C-1.5%Mn alloy. (a) Influence of Al addition; (b) Influence of Si addition

Fig. 4. Comparison of the influence of Al and Si additions on ferrite volume fraction and carbon content at 750 ºC, 800 ºC and 850 ºC for a Fe-0.15%C-1.5%Mn alloy. (a) Influence of Al addition; (b) Influence of Si addition

Fig. 5. Comparison of the influence of Al and Si additions on the carbon content of phases at 800 ºC for a Fe-0.15%C-1.5%Mn alloy. (a) Influence of Al and Si on austenite carbon content; (b) Influence of Al and Si on ferrite carbon content

Fig. 6. Comparison of the influence of Al and Si additions on the carbon content of phases at intercritical temperatures corresponding to 50% and 70% ferrite for a Fe-0.15%C-1.5%Mn alloy. (a) Influence of Al and Si on austenite carbon content; (b) Influence of Al and Si on ferrite carbon content

Fig. 7. Comparison of the effect of the addition of 1% Al or 1% Si to a Fe-0.15%C-1.5%Mn alloy in the temperature range (400 ºC-1000ºC). (a) Effect on austenite volume fraction; (b) Effect on ferrite volume fraction; (c) Effect on austenite carbon content; (d) Effect on ferrite carbon content. The temperatures corresponding to typical intercritical phase distributions with 50% ferrite and 70% ferrite are included in the figures.

Fig. 8. Comparison of the influence of 1% Al and 1% Si additions on the alloying element content (Al% or Si%) in austenite and ferrite for a Fe-0.15%C-1.5%Mn alloy in the temperature range (400 ºC-1000ºC).

Fig. 9. Comparison of the influence of Al and Si additions on the alloying element content (Al% or Si%) in austenite at intercritical temperatures corresponding to 50% and 70% ferrite for a Fe-0.15%C-1.5%Mn alloy.

Fig. 10. Comparison of the influence of 1% Al and 1% Si additions on the A_1 line and the limit of solubility of carbon in ferrite for a Fe-0.15%C-1.5%Mn alloy.

Fig. 11. Comparison of the effect of the addition of (0.5%-2%) Mn, (0%-1.5%) Al, (0%-1.5%) Si to the steel presented in **Table 2** on austenite volume fraction, austenite carbon content and carbon equivalent at 800 ºC calculated with Equation (1); a) Effect of Mn-Al combinations with 0% Si. b) Effect of Mn-Si combinations with 0% Al. c) Effect of Si-Al combinations with 1.5% Mn.

Fig. 12. Comparison of the influence of Al and Si additions on the hardenability of intercritical austenite at 800 ºC and at an intercritical temperature corresponding to 50% austenite. The steel analyzed is that presented in **Table 2** with 1.5% Mn. a) Carbon equivalent CE (determined with Eq. 1); b) Ideal critical diameter DI according to ASTM A 255-07 standard; c) Relationship between CE an DI.

Fig. 13. Comparison of the influence of Al and Si additions on the CCT diagram of the steel presented in **Table 2** with 1.5% Mn. Reheating temperature corresponding to 50% ferrite and 50% austenite. a) CMn grade without Al or Si; b) Influence of 1% Al; c) Influence of 1% Si; d) Curves for the start of ferrite formation with a cooling rate of 15 ºC/s. Ferrite transformation start (*Fs*) times and temperatures at 15 ºC/s are indicated for the three compositions.

Table 1. Chemical composition of the Fe-C-Mn-Al and Fe-C-Mn-Si model alloys used to study by means of JMatPro™ simulations the effect of Al and Si on the Fe-C-1.5% Mn phase diagram, the volume fractions of phases and the C, Al and Si contents in phases formed during annealing (wt%).

C	Mn	Si	Al
0-0.9	1.5	0-1.5	0-1.5

Table 2. Chemical composition of the model TRIP steel used to study by means of JMatPro™ simulations the effect of Mn, Al and Si additions on the austenite volume fraction and carbon equivalent at 800 ºC (wt%).

C	Mn	Si	Al	P	S	Cr	Mo	Cu	Ni	V	Nb	Ti	B	N
0.15	0.5-2	0-1.5	0-1.5	0.01	0.005	0.3	0.15	0	0	0	0.03	0.03	0	0.006

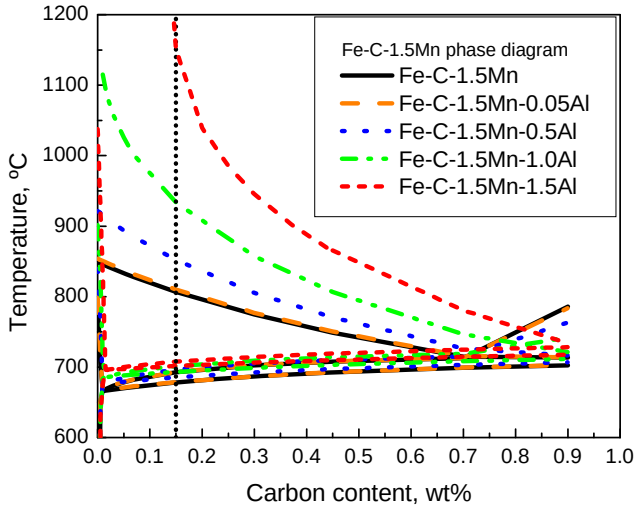

a)

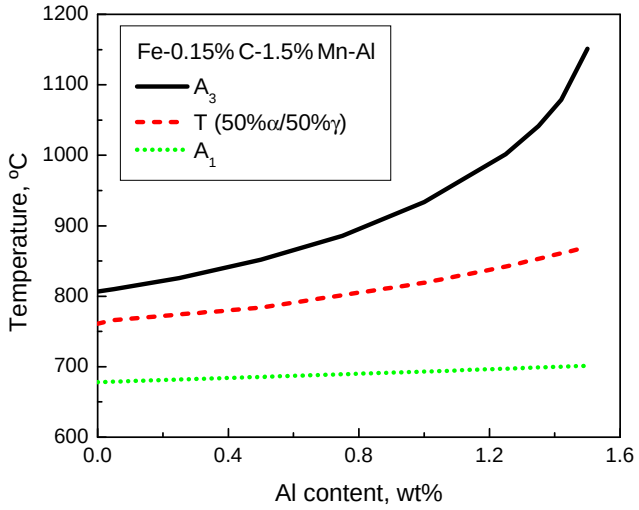

b)

Fig. 1. (a) Effect of Al additions (between 0% and 1.5% Al) on the transformation lines of Fe-C-1.5%Mn phase diagram; (b) Effect of Al on transformation temperatures for a Fe-0.15%C-1.5%Mn alloy. The temperatures represented are the austenite-ferrite transformation temperature (A_3), the temperature for a 50% austenite / 50% ferrite phase distribution and the eutectoid transformation temperature (A_1).

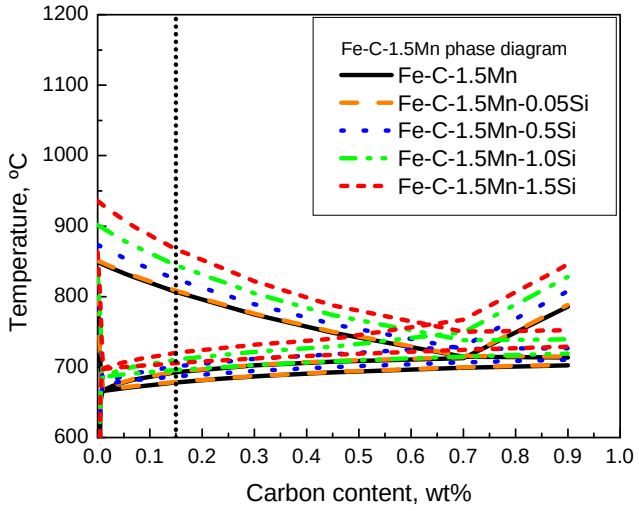

a)

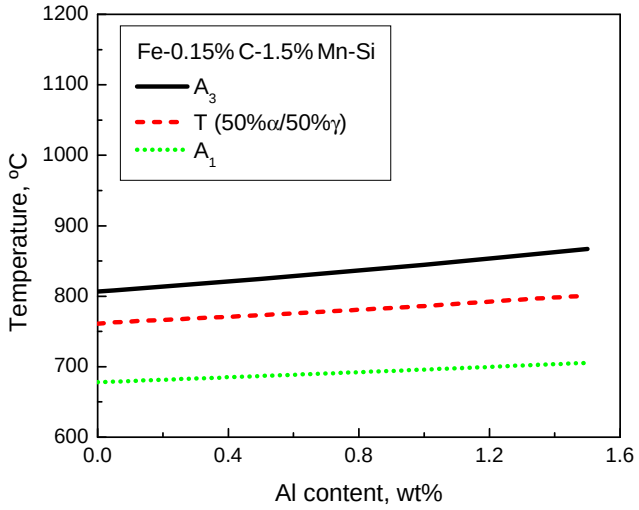

b)

Fig. 2. (a) Effect of Si additions (between 0% and 1.5% Si) on the transformation lines of Fe-C-1.5%Mn phase diagram; (b) Effect of Si on transformation temperatures for a Fe-0.15%C-1.5%Mn alloy. The temperatures represented are the austenite-ferrite transformation temperature (A_3), the temperature for a 50% austenite / 50% ferrite phase distribution and the eutectoid transformation temperature (A_1).

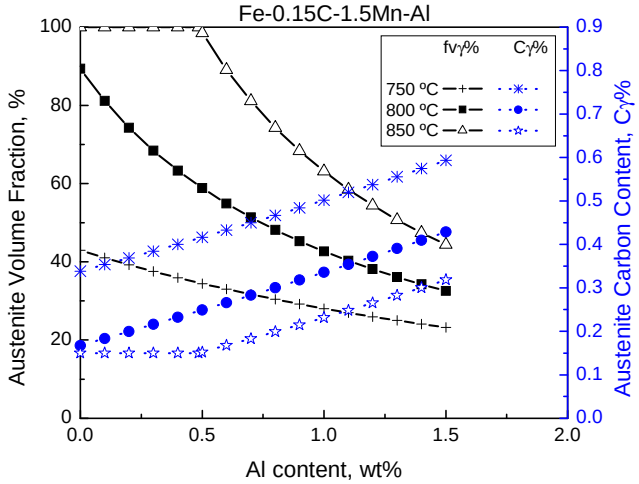

a)

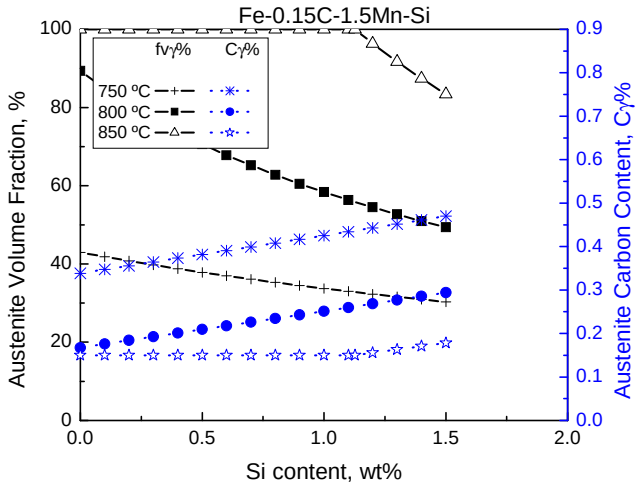

b)

Fig. 3. Comparison of the influence of Al and Si additions on austenite volume fraction and carbon content at 750 ºC, 800 ºC and 850 ºC for a Fe-0.15%C-1.5%Mn alloy. (a) Influence of Al addition; (b) Influence of Si addition

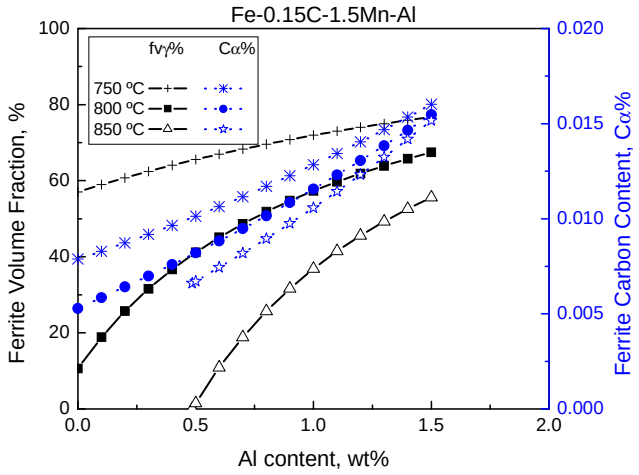

a)

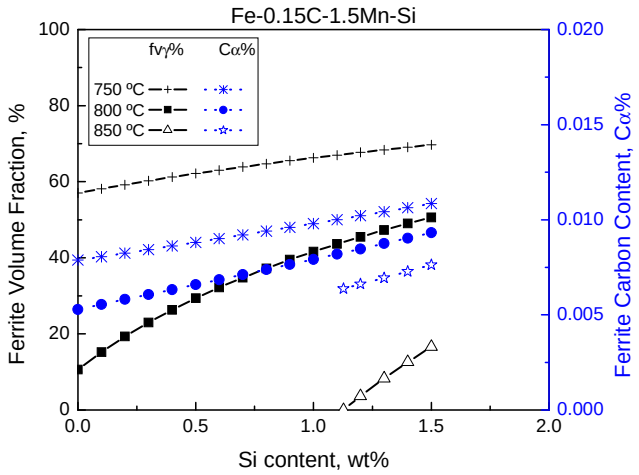

b)

Fig. 4. Comparison of the influence of Al and Si additions on ferrite volume fraction and carbon content at 750 ºC, 800 ºC and 850 ºC for a Fe-0.15%C-1.5%Mn alloy. (a) Influence of Al addition; (b) Influence of Si addition

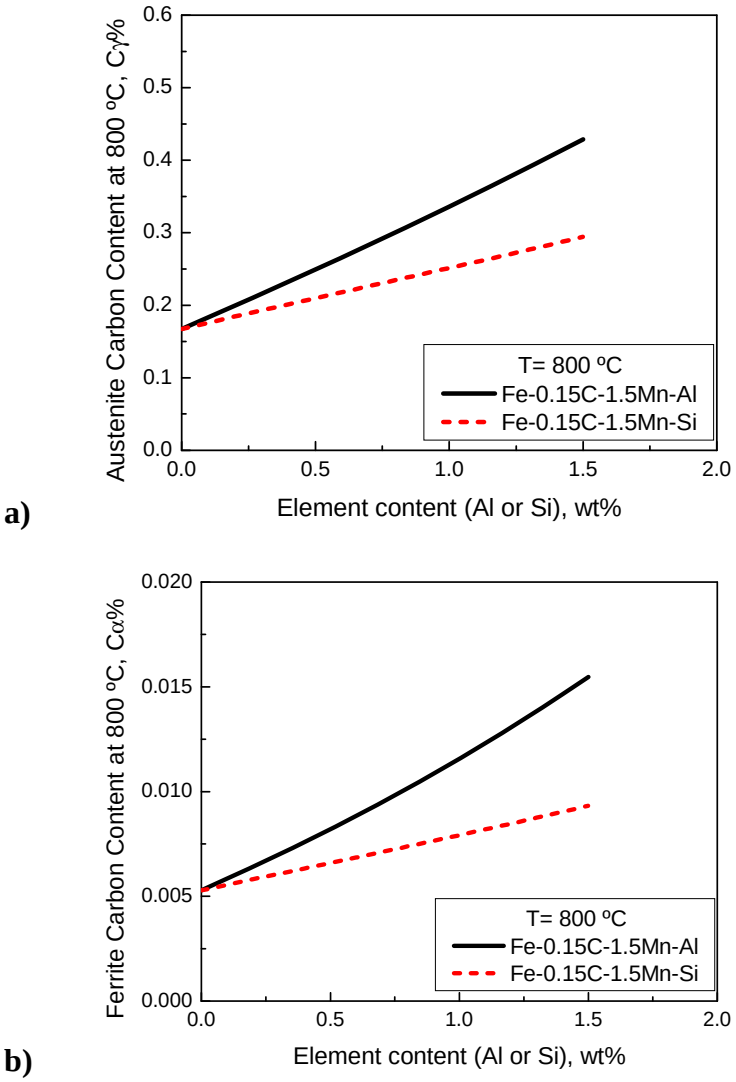

Fig. 5. Comparison of the influence of Al and Si additions on the carbon content of phases at 800 ºC for a Fe-0.15%C-1.5%Mn alloy. (a) Influence of Al and Si on austenite carbon content; (b) Influence of Al and Si on ferrite carbon content

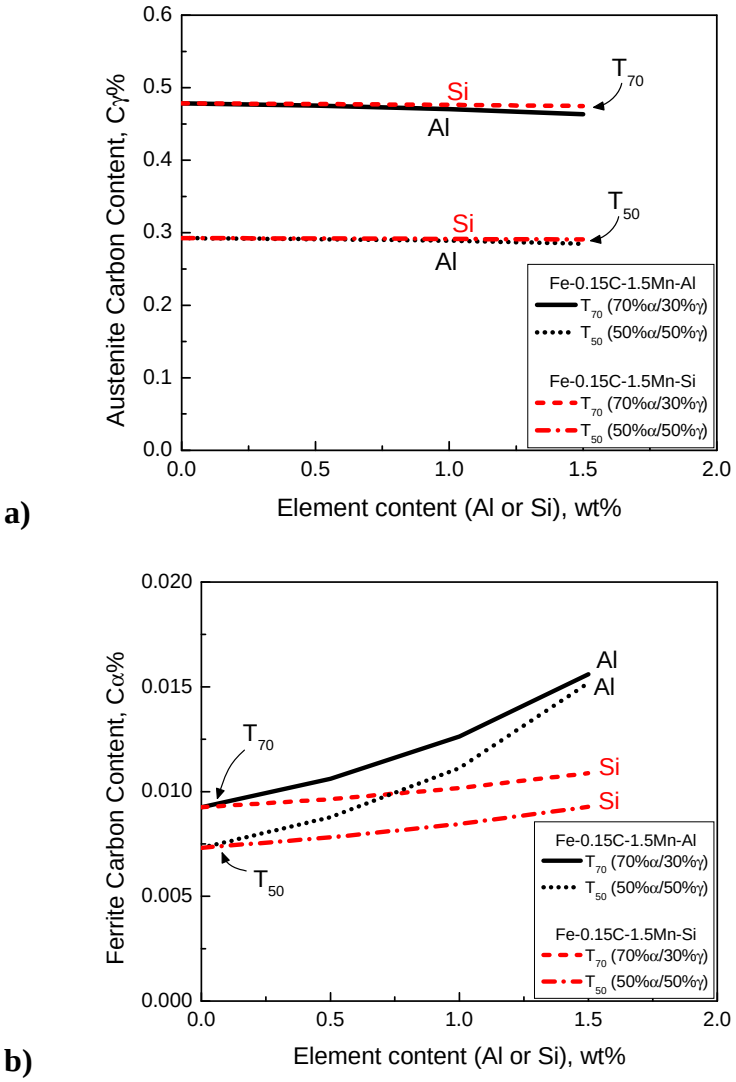

Fig. 6. Comparison of the influence of Al and Si additions on the carbon content of phases at intercritical temperatures corresponding to 50% and 70% ferrite for a Fe-0.15%C-1.5%Mn alloy. (a) Influence of Al and Si on austenite carbon content; (b) Influence of Al and Si on ferrite carbon content

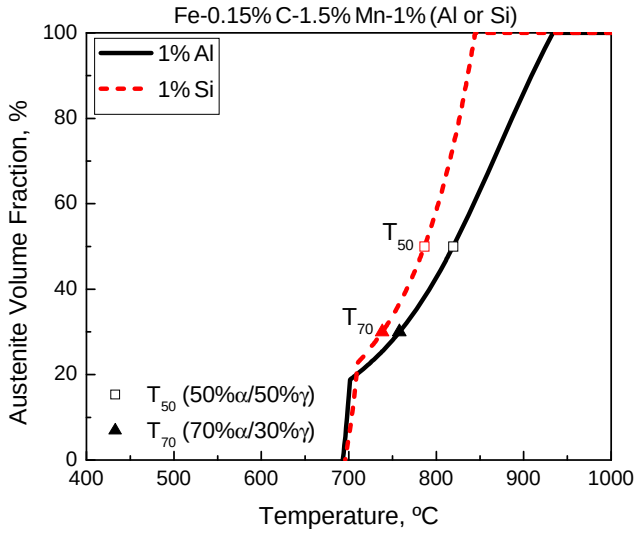
Fe-0.15% C-1.5% Mn-1% (Al or Si)
1% Al
1% Si
Austenite Volume Fraction, %
Temperature, ºC
T50
T70
T50 (50%α/50%γ)
T70 (70%α/30%γ)

a)

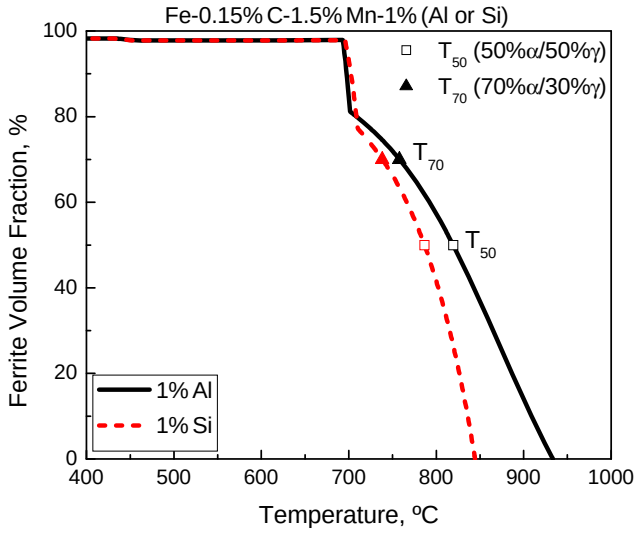
Fe-0.15% C-1.5% Mn-1% (Al or Si)
T50 (50%α/50%γ)
T70 (70%α/30%γ)
T70
T50
1% Al
1% Si
Ferrite Volume Fraction, %
Temperature, ºC

b)

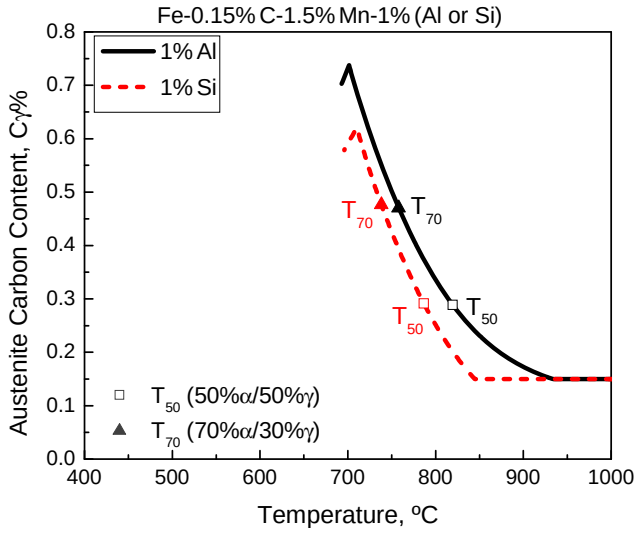
Fe-0.15% C-1.5% Mn-1% (Al or Si)
1% Al
1% Si
T70
T70
T50
T50
T50 (50%α/50%γ)
T70 (70%α/30%γ)
Austenite Carbon Content, Cγ%
Temperature, ºC

c)

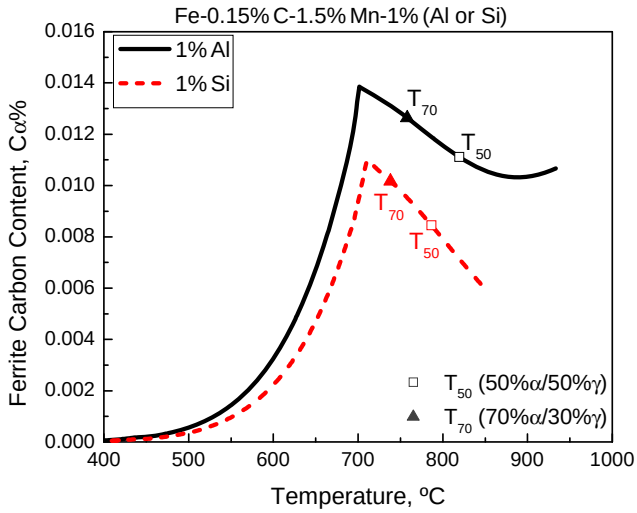

d)

Fig. 7. Comparison of the effect of the addition of 1% Al or 1% Si to a Fe-0.15%C-1.5%Mn alloy in the temperature range (400 ºC-1000ºC). (a) Effect on austenite volume fraction; (b) Effect on ferrite volume fraction; (c) Effect on austenite carbon content; (d) Effect on ferrite carbon content. The temperatures corresponding to typical intercritical phase distributions with 50% ferrite and 70% ferrite are included in the figures.

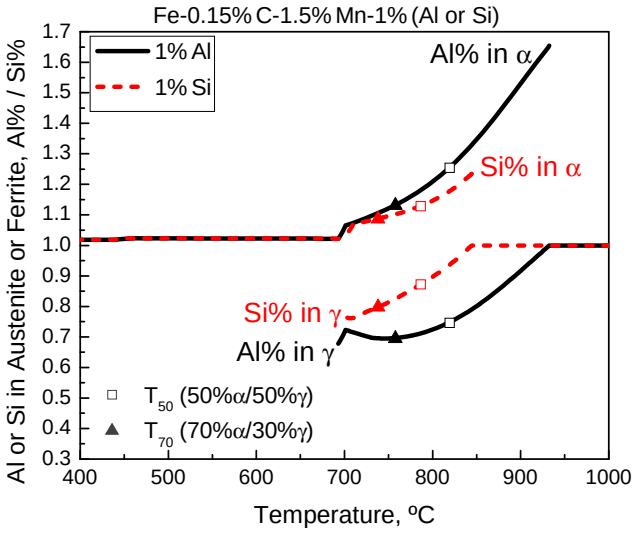

Fig. 8. Comparison of the influence of 1% Al and 1% Si additions on the alloying element content (Al% or Si%) in austenite and ferrite for a Fe-0.15%C-1.5%Mn alloy in the temperature range (400 ºC-1000ºC).

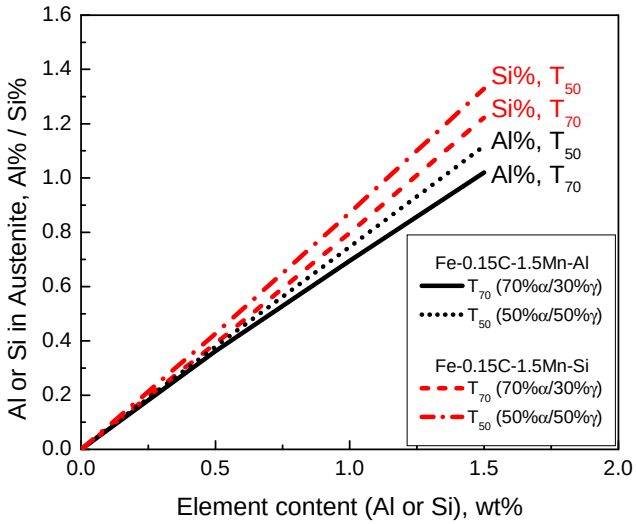

Fig. 9. Comparison of the influence of Al and Si additions on the alloying element content (Al% or Si%) in austenite at intercritical temperatures corresponding to 50% and 70% ferrite for a Fe-0.15%C-1.5%Mn alloy.

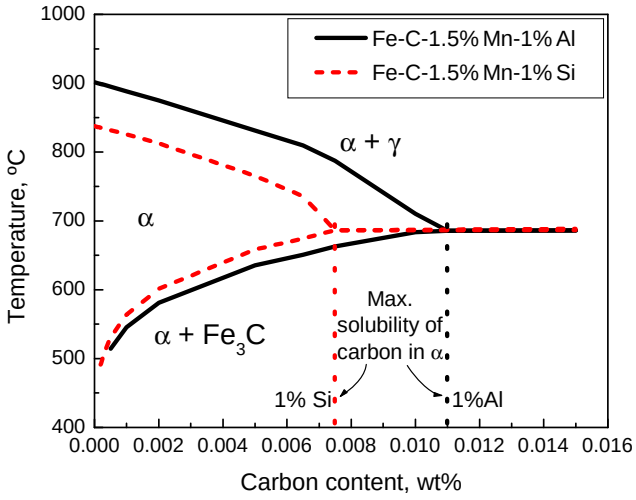

Fig. 10. Comparison of the influence of 1% Al and 1% Si additions on the A_1 line and the limit of solubility of carbon in ferrite for a Fe-0.15%C-1.5%Mn alloy.

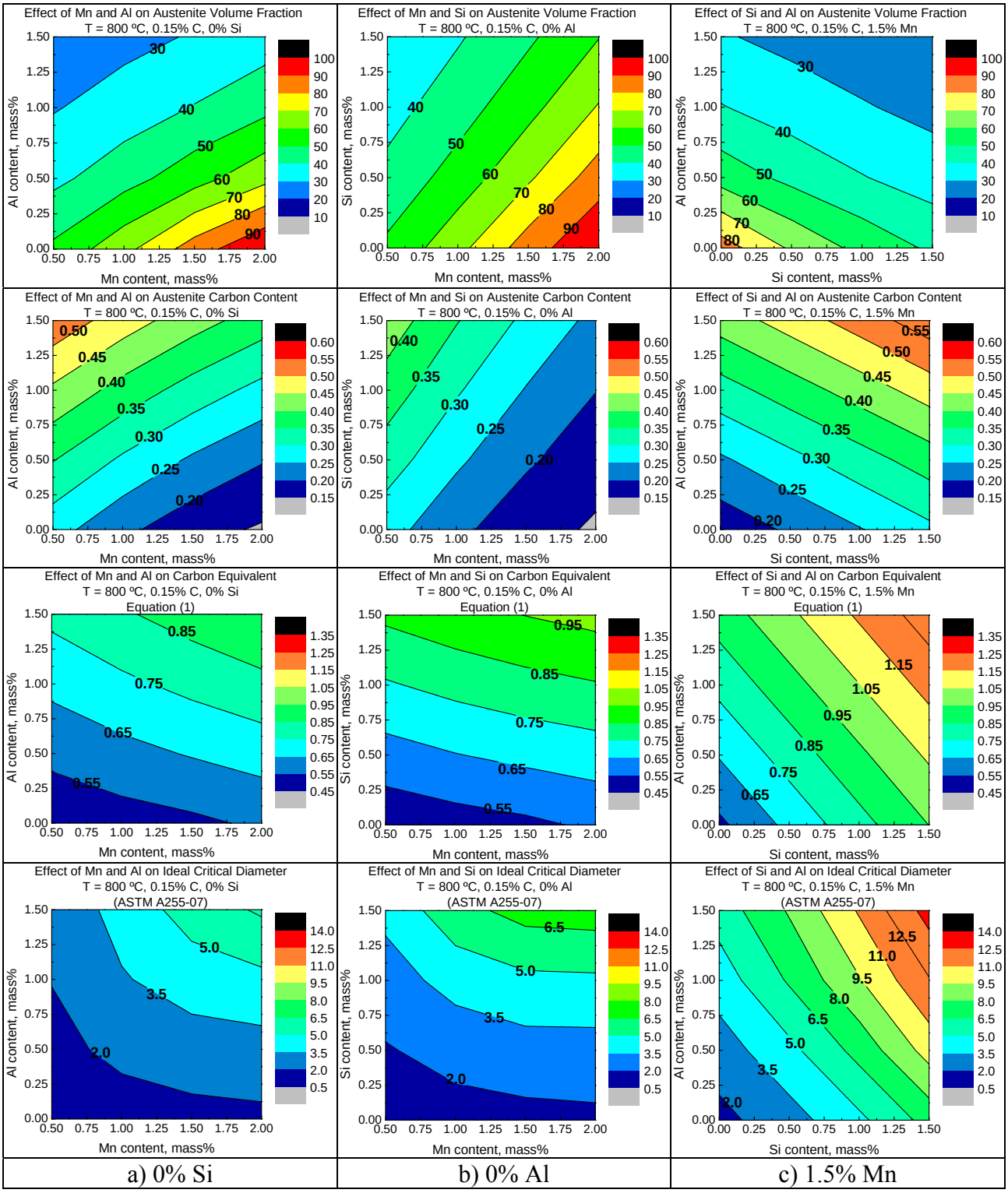

Fig. 11. Comparison of the effect of the addition of (0.5%-2%) Mn, (0%-1.5%) Al, (0%-1.5%) Si to the steel presented in **Table 2** on austenite volume fraction, austenite carbon content, carbon equivalent calculated with Equation (1) and ideal diameter

(DI) at 800 ºC; a) Effect of Mn-Al combinations with 0% Si. b) Effect of Mn-Si combinations with 0% Al. c) Effect of Si-Al combinations with 1.5% Mn.

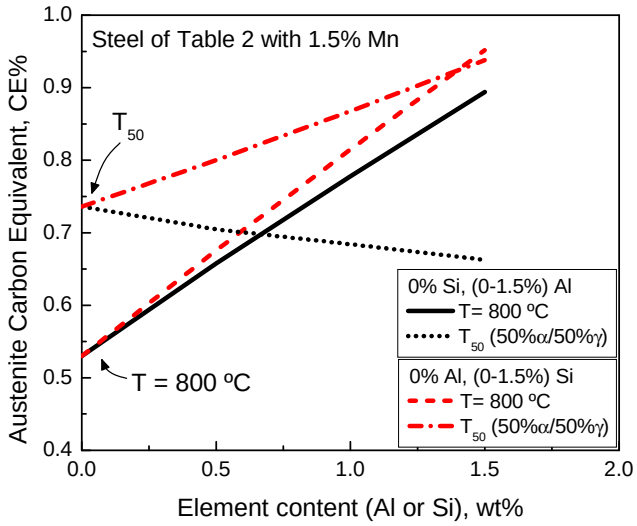

a)

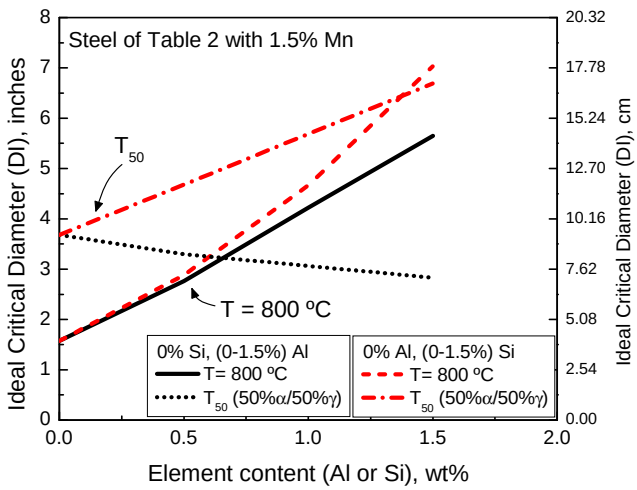

b)

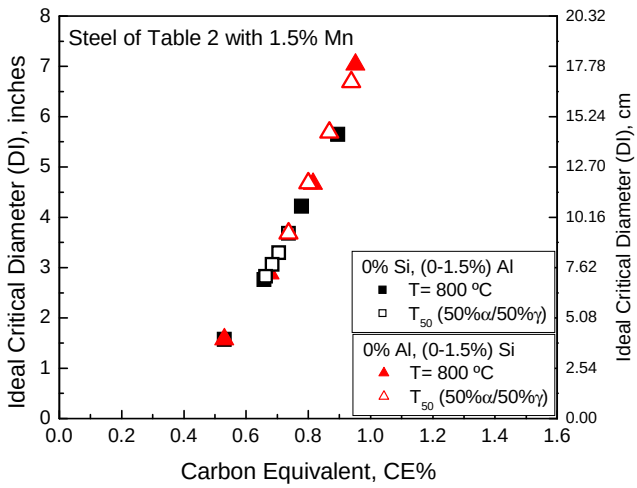

c)

Fig. 12. Comparison of the influence of Al and Si additions on the hardenability of intercritical austenite at 800 ºC and at an intercritical temperature corresponding

to 50% austenite. The steel analyzed is that presented in **Table 2** with 1.5% Mn. a) Carbon equivalent CE (determined with Eq. 1); b) Ideal critical diameter DI according to ASTM A 255-07 standard; c) Relationship between CE an DI.

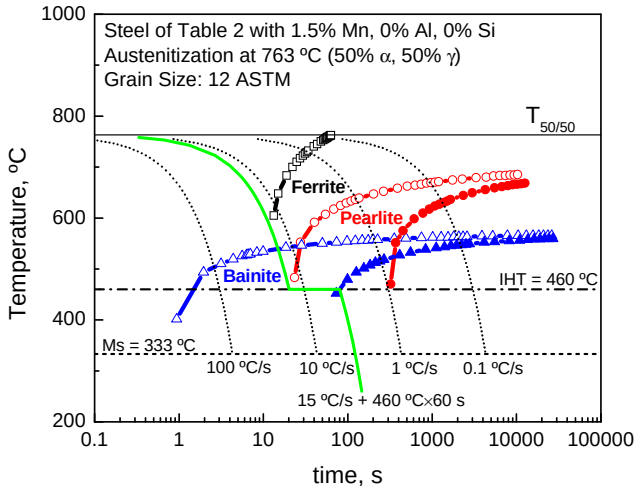
Steel of Table 2 with 1.5% Mn, 0% Al, 0% Si
Austenitization at 763 ºC (50% α, 50% γ)
Grain Size: 12 ASTM
T 50/50
Ferrite
Pearlite
Bainite
IHT = 460 ºC
Ms = 333 ºC
100 ºC/s
10 ºC/s
1 ºC/s
0.1 ºC/s
15 ºC/s + 460 ºC×60 s
Temperature, ºC
time, s

a)

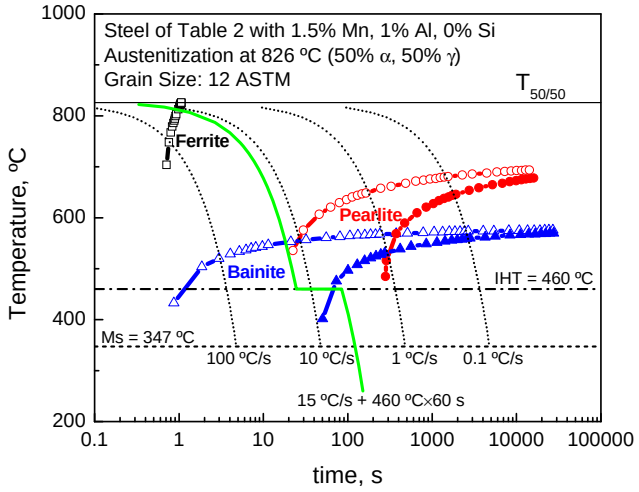
Steel of Table 2 with 1.5% Mn, 1% Al, 0% Si
Austenitization at 826 ºC (50% α, 50% γ)
Grain Size: 12 ASTM
T 50/50
Ferrite
Pearlite
Bainite
IHT = 460 ºC
Ms = 347 ºC
100 ºC/s
10 ºC/s
1 ºC/s
0.1 ºC/s
15 ºC/s + 460 ºC×60 s
Temperature, ºC
time, s

b)

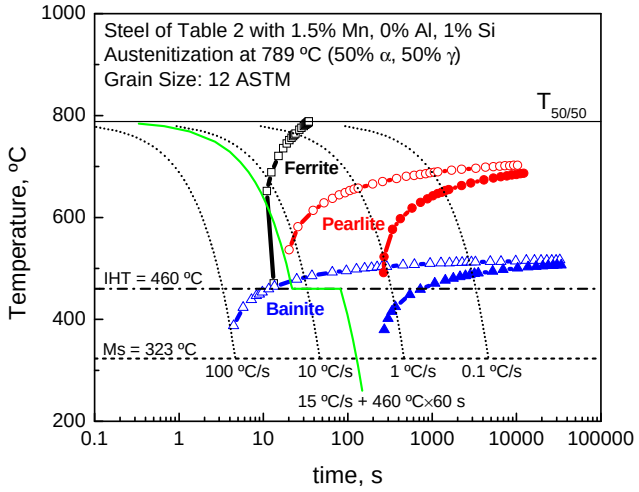
Steel of Table 2 with 1.5% Mn, 0% Al, 1% Si
Austenitization at 789 ºC (50% α, 50% γ)
Grain Size: 12 ASTM
T 50/50
Ferrite
Pearlite
Bainite
IHT = 460 ºC
Ms = 323 ºC
100 ºC/s
10 ºC/s
1 ºC/s
0.1 ºC/s
15 ºC/s + 460 ºC×60 s
Temperature, ºC
time, s

c)

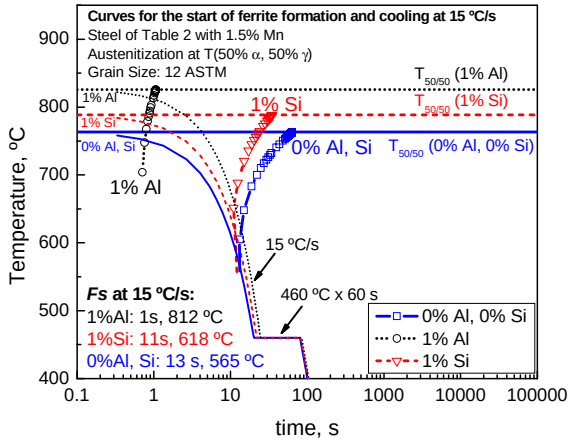

d)

Fig. 13. Comparison of the influence of Al and Si additions on the CCT diagram of the steel presented in **Table 2** with 1.5% Mn. Reheating temperature corresponding to 50% ferrite and 50% austenite. a) CMn grade without Al or Si; b) Influence of 1% Al; c) Influence of 1% Si; d) Curves for the start of ferrite formation with a cooling rate of 15 ºC/s. Ferrite transformation start (*Fs*) times and temperatures at 15 ºC/s are indicated for the three compositions.